Charge Confinement and Doping at $LaAlO_3/SrTiO_3$ Interfaces

T. Fix, F. Schoofs, J. L. MacManus-Driscoll, and M. G. Blamire

Department of Materials Science, University of Cambridge, Pembroke Street, Cambridge CB2 3QZ, United Kingdom

(Received 29 June 2009; published 16 October 2009)

The thickness and origin of the free charge layer which forms at the $LaAlO_3/SrTiO_3$ interface is still uncertain. By inserting Mn dopants at different distances from the interface we can locate the position of carriers within the $SrTiO_3$ surface layers. We show that the majority of the carriers in fully-oxygenated samples are confined within 1 unit cell of the interface. This confirms the ''polar-catastrophe'' mechanism proposed for this system but the low mobility of these carriers demonstrates the need for improved materials for applications and a more complete understanding of the role of the minority of higher mobility carriers identified.

DOI: 10.1103/PhysRevLett.103.166802 PACS numbers: 73.40.−c, 71.55.Gs, 72.20.Jv

The formation of conducting states at the interface between insulating oxides is currently one of the most topical areas of electronic materials research. Examples include the creation of a high density charge sheet between $SrTiO_3$ (STO) and $LaAlO_3$ (LAO) [1–3], the formation of ferromagnetism between the antiferromagnetic insulators $LaMnO_3$ and $SrMnO_3$ [4–6] and the appearance of superconductivity at the interface between nonsuperconducting La_2CuO_4 and $La_{1.64}Sr_{0.36}CuO_4$ [7]. The proposed mechanism underlying this behavior involves charge transfer to interface states leading to changes in cation valence. More prosaically, some aspects of the results appear to be partly explicable through the formation of oxygen vacancies or intermixing of cations at the interfaces [8,9]. In each of these systems therefore, fully determining the nature of the interfacial states and their origin is of high importance.

In the most studied system, the two-dimensional electron gas (2DEG) formed at the interface of an LAO film and a Ti-terminated STO substrate, the theoretical understanding is that (001) LAO is polar and so its growth on nonpolar (001) STO leads to a divergent surface potential with increasing thickness which can be eliminated by the transfer of half an electronic charge to the interfacial Ti ions. This results in the formation of a 2DEG [1]. Depending on the method of analysis, this charge is either confined to the first unit cell (uc) [10] of the STO or at least to within around 3 uc of the interface [11,12]. This view is supported by hard x-ray photoelectron spectroscopy [13] and by XPS [14], which place the Ti^{3+} states within 1 nm of the interface. Transport measurements have confirmed some aspects of this picture: most notably, many groups have shown that at least $\sim$5 uc of LAO is required to initiate the formation of the 2DEG and that further increases in thickness do not create additional carriers [15].

There are many aspects of the transport behavior of LAO/STO, however, which appear inconsistent with the charge transfer model. For example it is now accepted that LAO growth in a low oxygen pressure induces a high density of oxygen vacancies in the STO substrate which cannot be entirely eliminated by oxygen annealing [8,9]. STO oxygen vacancies are electron donors and the resulting conductivity has been measured directly by scanning probe microscopy of a cross-sectioned sample [16]. However, for samples grown at high oxygen pressures the apparent width of the charge sheet is reduced only to 7 nm, which is much larger than the thickness predicted by theory (although this may represent the resolution limit of the technique). The less invasive technique of measuring the anisotropy of the upper critical field of superconducting samples has also yielded 7–10 nm as the probable thickness of the free charge layer [17].

There seems to be a puzzling dichotomy emerging, with chemical data and theoretical predictions pointing to an intrinsic two-dimensional charge sheet and transport data to a larger thickness which could be explained in conventional semiconductor terms by band bending and the formation of an interfacial conduction band minimum [18], possibly in combination with doping by oxygen vacancies.

Conventional Hall effect measurements which are normally used to determine the properties of the 2DEG carriers cannot easily resolve this issue because they provide information only on the areal carrier density. In a recent paper we reported substantial depression of this carrier density in 2DEGs formed when a transition metal-doped layer of STO is grown homoepitaxially on the STO substrate and capped with the conventional LAO layer [19]; in particular, the carrier density was strongly suppressed by the addition of even a single uc of Mn-doped STO at the LAO interface. In this paper we report on experiments in which delta-doped layers are inserted at different positions within an STO homoepitaxial layer. The results demonstrate the recovery of the measured carrier concentration and mobility as soon as even a single uc of undoped STO is placed at the LAO interface. We demonstrate, via a simple model of the carrier density, that this implies that the majority of the carriers are confined to the first STO unit cell.

Films were grown on Ti-terminated single-crystal STO substrates by pulsed laser deposition (PLD) using a KrF laser with a 248 nm wavelength. The growth conditions

 © 2009 The American Physical Society

were 10 Hz repetition rate, and a fluence of around $1\ \mathrm{J\,cm^{-2}}$ on the target at a substrate target distance of 80 mm; the heater temperature was 850 °C and the oxygen pressure while depositing and cooling down was around 10^{-2} mBar of O_2 which is above the threshold for the introduction of a high density of oxygen vacancies [20]. Commercial LAO and STO targets were used while $SrTi_{0.98}Mn_{0.02}O_3$ (Mn-STO) targets for doping were made by milling, presintering at 900 °C for 6 h, pressing and sintering at 1300 °C for 6 h a stoichiometric mixture of high purity (99.99%) $SrCO_3$, TiO_2, and MnO_2 powders. All the films were grown in 2D mode and the spot intensity of the reflective high-energy electron diffraction (RHEED) pattern was monitored *in situ*. Well-defined RHEED oscillations were observed in all conditions indicating layer-by-layer growth and allowing accurate control of the number of unit cells deposited.

In [19] we demonstrated that the properties of 2DEGs were sensitive even to the addition of undoped STO layers to the substrate and so in order to appreciate the effects of the location of the Mn dopants it is important that comparison is made with samples consisting of similar numbers of unit cells of undoped homoepitaxial STO. Figure 1 shows the sample structures used in these experiments which are heterostructures consisting of $STO_{substrate}$/Mn-STO(M uc)/STO(L uc)/LAO(15 uc). A standard 2DEG formed by the growth of 15 uc LAO on STO substrates (i.e. L, $M = 0$) was taken as a reference for the other experiments, and it carrier density and mobility are comparable with samples grown under similar conditions elsewhere. Electrical contacts were made with an Al wire bonder, the resistivity was measured using a four-probe technique and the Hall effect in a van der Pauw configuration to extract the sheet carrier density and mobility.

Figure 2 shows the carrier density and mobility at 200 K for a series of samples plotted versus the total number of homoepitaxial STO layers $N = L + M$. 30 nm thick epitaxial films of Mn-STO were insulating and so we ascribe the conductivity in all cases to the presence of the interface. For comparison, we have reproduced the data for $M = 0$ (undoped STO) from [19] in Fig. 2(a); this shows a progressive decline in carrier density with increasing N but little significant change in mobility. The decline observed probably originates from the much higher density of defects present in homoepitaxial STO films compared with single-crystal substrates (see, for example, [21,22]). These defects originate from a variety of sources: nonstoichiometry and imperfect growth nucleation coupled with ion damage from high-energy particles from the laser plume. In Fig. 2(b) we show that the carrier densities of the interfacially doped samples ($L = 0$) lie well below the equivalent $M = 0$ samples with the same N while the opposite is true for the mobility which is significantly enhanced. In contrast, for the offset-doped samples (M, $L \geq 1$) samples in which the Mn-doped layer is separated from the STO/LAO interface by at least 1 uc of undoped STO, the carrier densities for low N are at least as high as for the undoped ($M = 0$) samples while the mobility drops back to the low values measured for the undoped samples [Fig. 2(c)]. With increasing N the mobility and carrier density of all the samples tend towards the same values.

Figure 3 shows resistance vs temperature ($R(T)$) for a number of the samples. The resistivity was measured along [100] STO for a $10 \times 5\ \mathrm{mm}^2$ substrate; the IV curves were rather linear so that the current was tuned for each sample in order to measure a wide range of resistivity. There is a degree of scatter in the low temperature data, but for $N \geq 5$

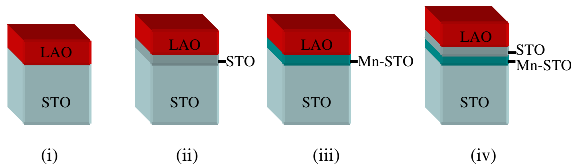

FIG. 1 (color online). Schematic diagrams of the samples grown for these experiments. (i) Reference $LaAlO_3/SrTiO_3$ (substrate); (ii) L layers of homoepitaxial $SrTiO_3$ grown between the substrate and the $LaAlO_3$ cap; (iii) M layers of Mn-doped $SrTiO_3$ grown between the substrate and the $LaAlO_3$ cap; (iv) $N(= L + M)$ layers grown on the $SrTiO_3$ substrate so that the LAO/STO interface is formed between $LaAlO_3$ and undoped homoepitaxial $SrTiO_3$.

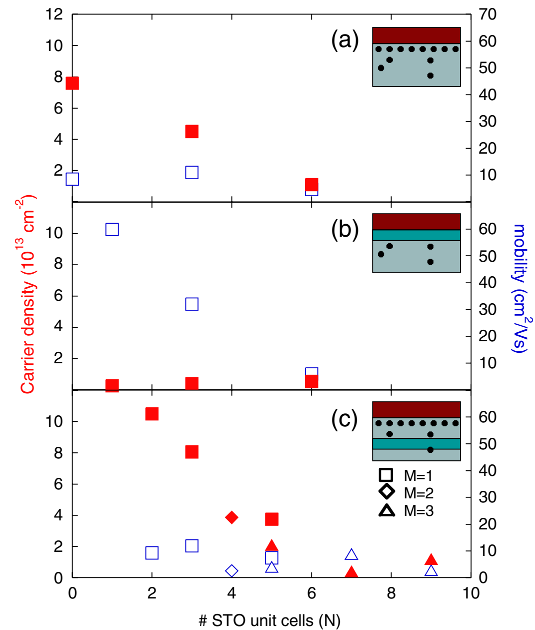

FIG. 2 (color online). Areal carrier density (red/solid symbols) and mobility (blue/open symbols) measured at 200 K for $STO_{substrate}$/Mn-STO(M uc)/STO(L uc)/LAO(15 uc) heterostructures versus total number of homoepitaxial layers N: (a) undoped ($M = 0$, $L = N$) samples (from [19]); (b) interfacially doped samples ($L = 0$, $M = N$); (c) off-set doped samples ($L + M = N$) with different values of M as marked in the key. The inset schematic diagrams indicate the position of the Mn-doped layer within the heterostructure and the carrier density distribution inferred from our results.

the resistance strongly increases with decreasing temperature implying that defects in the heteroepitaxial STO strongly localize carriers at low temperature.

It is clear from Fig. 2 that the position of the Mn dopants critically determines the properties of the interfacial 2DEG. The primary effect appears in the $L = 0$ samples where the dopants lie at the LAO/STO interface [Fig. 2(b)]: here the carrier density is greatly reduced with a corresponding rise in the measured Hall mobility relative to the $M = 0$ control samples. This effect is eliminated by the insertion of undoped STO at the interface ($L \geq 1$), thereby recreating a clean STO/LAO interface; here the carrier density increases to levels comparable (or even exceeding) the values for $M = 0$ and shows a similar decrease with N [Fig. 2(c)]. We will show below that this behavior can be explained directly by the assumption of two distinct carrier types within the 2DEG. Such a separation of carriers into two different subbands has been recently predicted by Popovic *et al.* [11] on the basis of density functional theory calculations. Their results suggest that the majority of the carriers are confined to the first unit cell in a deep subband, with a lower density extending through the next few Ti layers as a result of local polarization of the STO. The former (which we term type I) are expected to have a largely two-dimensional character, a large effective mass and the possibility of forming self-trapped polarons, while the latter (type II) exist in more three-dimensional subbands, and have lower effective masses with correspondingly larger mobilities. The cartoons inset to Fig. 2 illustrate the positions of the dopants in the various types of samples measured and their relation to the inhomogeneous charge density.

We start our treatment of our results with the assumption that the effect of a Mn dopant is entirely confined to the Ti layer into which it substitutes. The relative sizes [23] suggest that Mn^{3+} should substitute for Ti^{4+} and Mn^{2+} for the Ti^{3+} induced by charge transfer. In both cases therefore the Mn thus acts as an electron acceptor and, since the Mn ion size is smaller than the corresponding Ti ion, substitution may promote the local distortion and polaron formation postulated by Popvic *et al.* [11]. On this basis the large reduction observed by us in carrier densities induced by Mn-doping at the interface could be explained by the trapping of the type I carriers leaving a lower density of higher mobility type II carriers.

We therefore adopt a highly simplified model for the electrical properties of our reference 2-DEG such that Mn-doping traps all the carriers within a particular layer and that the properties can be explained in terms of two independent carrier types. We adapt the standard Hall effect expressions for carrier density and mobility in the presence of two distinct carrier types so that the measured areal carrier density n and mobility μ are given by

$$n = \frac{(n_{\rm I}\mu_{\rm I} + n_{\rm II}\mu_{\rm II})^2}{n_{\rm I}{\mu_{\rm I}}^2 + n_{\rm II}{\mu_{\rm II}}^2}, \qquad \mu = \frac{n_{\rm I}{\mu_{\rm I}}^2 + n_{\rm II}{\mu_{\rm II}}^2}{n_{\rm I}\mu_{\rm I} + n_{\rm II}\mu_{\rm II}}, \quad (1)$$

where $n_{\rm I(II)}$ and $\mu_{\rm I(II)}$ are, respectively, the areal carrier density and mobility of the type I (II) electrons. The scattering of the type II carriers occurs both in the interfacial unit cell and within the adjacent STO layers and so we can further decompose the mobility of type II carriers so that

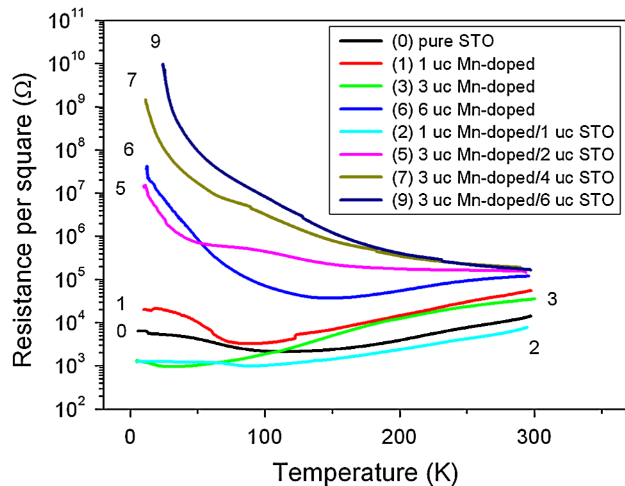

FIG. 3 (color online). Resistance versus temperature for $STO_{substrate}$/Mn-STO(M uc)/STO(L uc)/LAO(15 uc) heterostructures (N).

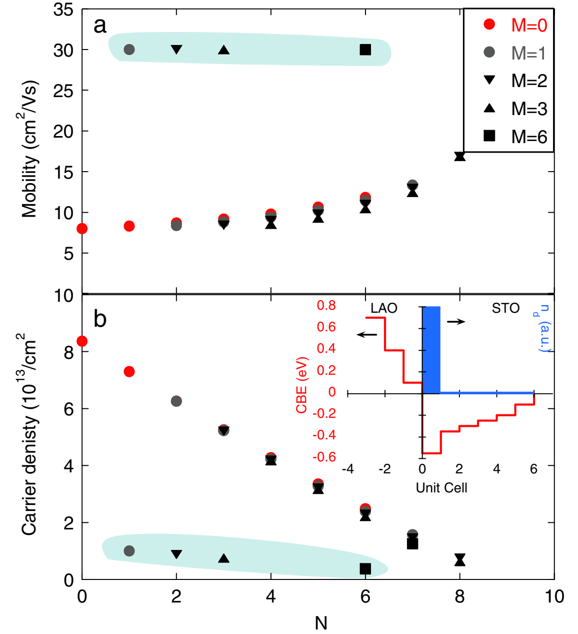

FIG. 4 (color online). Modeled mobility (a) and areal carrier density (b) data; the different symbols relate to different numbers of Mn-STO (M) as indicated in the legend. Interfacially doped samples ($M \geq 1$) without a STO interlayer ($L = 0$) lie within the shaded region of the plots. Inset shows the calculated position of the conduction band edge (CBE) from Ref. [11] and the inferred carrier density from our modeled data for each unit cell in the LAO/STO heterostructure.

$$\mu_{\rm II} = \frac{d}{1/\mu''_{\rm II} + (d-1)/\mu'_{\rm II}} : L \neq 0,\ M \neq 0, \qquad (2)$$
$$\mu_{\rm II} = \mu'_{\rm II} : L = 0,\ M \geq 1,$$

where d is the thickness in unit cells of the type II charge sheet and $\mu'_{\rm II}$ is the intrinsic mobility of the carriers within the STO. The top expression in (2) applies if the STO/LAO interface is not Mn-doped and the latter if only type II carriers are present and are confined away from the interface.

Using this model, we can create plots of the mobility and carrier density as shown in Fig. 4. As can be seen, the overall form of the results shown in the corresponding plots in Fig. 2 is well reproduced with the $L = 0$ samples being distinct from the remainder; the values used for the modelling were $n_{\rm I} = 1 \times 10^{14}$ cm^{-2} [24], $n_{\rm II} = 1 \times 10^{13}$ cm^{-2}, $\mu_{\rm I}$, $\mu''_{\rm II} = 5$ cm^2 V^{-1} s^{-1}, and $\mu'_{\rm II} = 30$ cm^2 V^{-1} s^{-1}. The first three values were chosen to provide reasonable agreement with the experimental data, but $\mu_{\rm II}$ was taken from Ohtomo and Hwang [1] for samples grown at low oxygen pressures in which the majority of carriers are now understood to exist within the substrate and so should reflect the intrinsic mobility of STO. This argument is strengthened by difference in the behavior of the mobility between Figs. 2(a) and 4(a): in the experimental results the overall mobility of the $L = 0$ samples declines with N, presumably due to increased scattering from defects such as dislocations [25] in the homoepitaxial STO so that the convergence of the $M = 6$ sample with the remainder of the data implies that the thickness of the type II charge sheet is of the order of 6 unit cells (i.e., when all the carriers are then confined within the more defective deposited material).

The inset to Fig. 4 illustrates the form of the model used: a large majority of the total carriers are confined to the first STO unit cell with a low density of highly mobile carriers extending a few unit cell further into the STO. This plot also shows the position of the conduction band edge calculated by Popovic *et al.* [11] which illustrates the predicted confinement of the two carrier types.

In this Letter we have used delta doping of Mn to distinguish between interfacial and "bulk" carriers and so have provided direct confirmation of the "polar-catastrophe" model for the formation of oxide 2-DEGs. Our results directly show that the majority of the carriers (type I) lie in the first unit cell from the interface but their mobility is low. The remaining carriers (type II) that penetrate further into the STO are of lower concentration but higher mobility, particularly in the case where the STO is a bulk single crystal. What is unclear at this stage is whether the type II carriers identified in our experiments are intrinsic or associated with oxygen vacancies induced during film growth as suggested by Herranz *et al.* [26]. However, our results suggest that with our growth conditions they are confined within 2–3 nm at the interface and so the values of up to 10 nm for the charge sheet thickness deduced from superconducting samples deposited at rather lower oxygen pressures [17] may suggest a prominent role for oxygen vacancy-donated electrons in such samples.

This work was supported by the EU Framework 6 Program NANOXIDE "Novel Nanoscale Devices based on functional Oxide Interfaces." We are grateful to Chris Bell and Alexey Kalabukhov for valuable suggestions.

[1] A. Ohtomo and H. Y. Hwang, Nature (London) **427**, 423 (2004).
[2] N. Reyren *et al.*, Science **317**, 1196 (2007).
[3] M. Huijben, A. Brinkman, G. Koster, G. Rijnders, H. Hilgenkamp, and D. H. A. Blank, Adv. Mater. **21**, 1665 (2009).
[4] T. Koida, M. Lippmaa, T. Fukumura, K. Itaka, Y. Matsumoto, M. Kawasaki, and H. Koinuma, Phys. Rev. B **66**, 144418 (2002).
[5] N. Ogawa, T. Satoh, Y. Ogimoto, and K. Miyano, Phys. Rev. B **78**, 212409 (2008).
[6] B. R. K. Nanda and S. Satpathy, Phys. Rev. Lett. **101**, 127201 (2008).
[7] S. Smadici, J. C. T. Lee, S. Wang, P. Abbamonte, G. Logvenov, A. Gozar, C. D. Cavellin, and I. Bozovic, Phys. Rev. Lett. **102**, 107004 (2009).
[8] G. Herranz *et al.*, Phys. Rev. Lett. **98**, 216803 (2007).
[9] A. Kalabukhov, R. Gunnarsson, J. Borjesson, E. Olsson, T. Claeson, and D. Winkler, Phys. Rev. B **75**, 121404 (2007).
[10] R. Pentcheva and W. E. Pickett, Phys. Rev. B **74**, 035112 (2006).
[11] Z. S. Popovic, S. Satpathy, and R. M. Martin, Phys. Rev. Lett. **101**, 256801 (2008).
[12] K. Janicka, J. P. Velev, and E. Y. Tsymbal, Phys. Rev. Lett. **102**, 106803 (2009).
[13] M. Sing *et al.*, Phys. Rev. Lett. **102**, 176805 (2009).
[14] M. Salluzzo *et al.*, Phys. Rev. Lett. **102**, 166804 (2009).
[15] S. Thiel, G. Hammerl, A. Schmehl, C. W. Schneider, and J. Mannhart, Science **313**, 1942 (2006).
[16] M. Basletic *et al.*, Nature Mater. **7**, 621 (2008).
[17] N. Reyren, S. Gariglio, A. D. Caviglia, D. Jaccard, T. Schneider, and J.-M. Triscone, Appl. Phys. Lett. **94**, 112506 (2009).
[18] K. Yoshimatsu, R. Yasuhara, H. Kumigashira, and M. Oshima, Phys. Rev. Lett. **101**, 026802 (2008).
[19] T. Fix, J. L. McManus-Driscoll, and M. G. Blamire, Appl. Phys. Lett. **94**, 172101 (2009).
[20] A. Brinkman *et al.*, Nature Mater. **6**, 493 (2007).
[21] A. Ohtomo and H. Y. Hwang, J. Appl. Phys. **102**, 083704 (2007).
[22] Y. Y. Tse, Y. Koutsonas, T. J. Jackson, G. Passerieux, and I. P. Jones, Thin Solid Films **515**, 1788 (2006).
[23] R. D. Shannon, Acta Crystallogr. Sect. E **32**, 751 (1976).
[24] To reproduce the observed behavior the value of n_I was linearly decreased with increasing N which is consistent with increased disorder-induced localization in thicker, more defective films.
[25] S. Thiel, C. W. Schneider, L. F. Kourkoutis, D. A. Muller, N. Reyren, A. D. Caviglia, S. Gariglio, J. M. Triscone, and J. Mannhart, Phys. Rev. Lett. **102**, 046809 (2009).
[26] G. Herranz *et al.*, Appl. Phys. Lett. **94**, 012113 (2009).